



## Experimental Entanglement Distribution by Separable States

Christina E. Vollmer,<sup>1</sup> Daniela Schulze,<sup>1</sup> Tobias Eberle,<sup>1</sup> Vitus Händchen,<sup>1</sup> Jaromír Fiurášek,<sup>2</sup> and Roman Schnabel<sup>1,\*</sup>

<sup>1</sup>*Institut für Gravitationsphysik, Leibniz Universität Hannover and Max-Planck-Institut für Gravitationsphysik (Albert-Einstein-Institut), Callinstrasse 38, 30167 Hannover, Germany*

<sup>2</sup>*Department of Optics, Palacký University, 17. listopadu 12, 77146 Olomouc, Czech Republic*

(Received 21 June 2013; published 4 December 2013)

Distribution of entanglement between macroscopically separated parties is crucial for future quantum information networks. Surprisingly, it has been theoretically shown that two distant systems can be entangled by sending a third system that is not entangled with either of them. Here, we experimentally distribute entanglement and successfully prove that our transmitted light beam is indeed not entangled with the parties' local systems. Our work demonstrates an unexpected variant of entanglement distribution and improves the understanding necessary to engineer multipartite quantum networks.

DOI: [10.1103/PhysRevLett.111.230505](https://doi.org/10.1103/PhysRevLett.111.230505)

PACS numbers: 03.67.Bg, 03.67.Hk, 42.50.Dv, 42.50.Ex

Entanglement is a fundamental resource for quantum information processing [1,2]. When a quantum protocol is intended to be executed between remote parties, entanglement distribution becomes the crucial issue. Let us consider the simplest case of two parties, often called Alice and Bob. Usually, the distribution of bipartite entanglement is performed by generating the entangled modes at Alice's place and sending one of the modes to the distant party Bob. Thereby, the mode sent from Alice to Bob is obviously entangled with the mode kept by Alice. It was thus a surprise when Cubitt *et al.* [3] theoretically showed that if more than two modes are involved, bipartite entanglement can also be distributed by sending fully separable states. This remarkable and seemingly paradoxical protocol is made possible by a specific structure of quantum correlations within an underlying state of three modes  $A$ ,  $B$ , and  $C$ . The protocol demands the state to be separable with respect to the  $B|AC$  and  $C|AB$  splittings and to be inseparable with respect to the  $A|BC$  splitting. According to the classification introduced in Ref. [4], entanglement distribution with separable states requires a three-mode entangled state belonging to class III. The protocol by Cubitt *et al.* [3], including further analysis done in Refs. [5,6], considered discrete variables. Mišta and Korolkova recently showed that entanglement distribution by separable states is also possible for continuous variables [7].

Here, we report on the experimental realization of entanglement distribution by separable states in the regime of continuous variables. Our experiment is in direct analogy to the original discrete-variable protocol as proposed in Ref. [3]. The principle of the protocol is illustrated in Fig. 1. In the beginning of the protocol, Alice possesses two separable modes  $A$  and  $C$ , while Bob possesses mode  $B$ , which is separable from Alice's modes. In the subsequent step I, Alice sends the ancillary mode  $C$ , which is neither entangled with mode  $A$  nor with mode  $B$ , to Bob. To obtain two-mode entanglement (step II), Bob mixes his modes  $B$  and  $C$ . One output mode is then discarded,

while the other one turns out to be entangled with  $A$ . The distributed entanglement can be used for further quantum information protocols [8], such as quantum teleportation [9,10] and quantum key distribution [11]. Our protocol explores the rich structure of multimode entanglement, which can exhibit more complex properties and features than two-mode entanglement and which represents a valuable resource for lots of applications ranging from local realism tests [12] to one-way quantum computing [13–15].

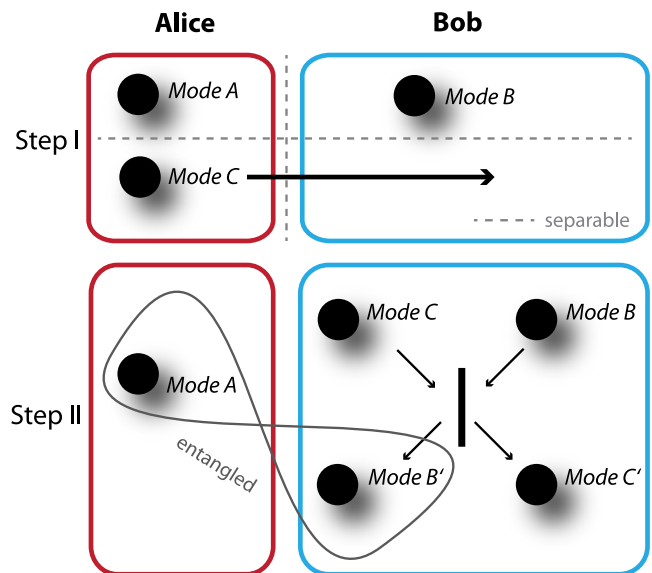


FIG. 1 (color online). Principle of entanglement distribution by separable states. In the beginning, Alice possesses two separable modes  $A$  and  $C$ . Both modes are also separable with respect to Bob's mode  $B$ . Alice sends mode  $C$  to Bob, and he combines his mode  $B$  with the received mode  $C$ . Finally, Alice and Bob share an entangled system  $A|B'$ , which can be traced back to the initial entanglement for the  $A|BC$  splitting.

Our setup for entanglement distribution by separable states is depicted in Fig. 2. The initial three-mode Gaussian state is prepared by an independent source and is distributed between Alice and Bob. The preparation starts with a squeezed state, which interferes with a vacuum state at a balanced beam splitter. The beam splitter output  $A$  is sent directly to Alice, while the other output is superimposed with a thermal state at a second balanced beam splitter. After the state preparation, Alice possesses modes  $A$  and  $C$ , while Bob holds mode  $B$ . The separability properties of this three-mode state ( $ABC$ ) are checked by a tomographic reconstruction of the full three-mode covariance matrix with the balanced homodyne detectors  $BHD_A$ ,  $BHD_B$ , and  $BHD_C$  and found to be separable with respect to the  $B|AC$  and  $C|AB$  splittings. In the next step, Alice sends mode  $C$  to Bob, where modes  $B$  and  $C$  interfere at a balanced beam splitter with the appropriate phase to get rid of the correlated noise. This step creates two-mode entanglement between Alice and Bob, which is verified by measuring the criterion by Duan *et al.* [16]

$$\text{Var}(\hat{X}_A - \hat{X}_{B'}) + \text{Var}(\hat{P}_A + \hat{P}_{B'}) < 4 \quad (1)$$

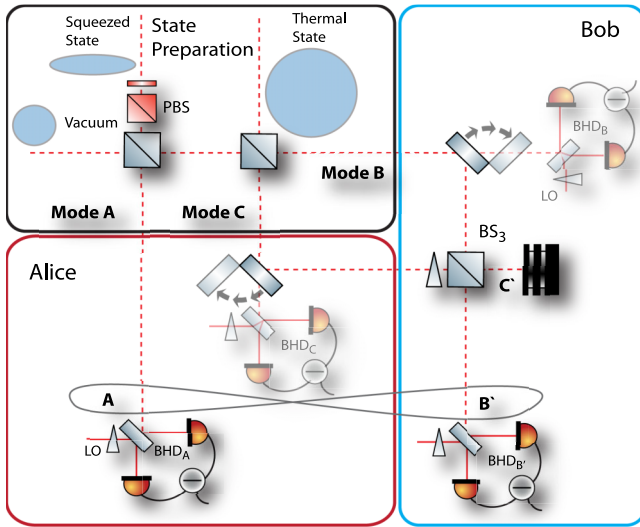


FIG. 2 (color online). Experimental setup for entanglement distribution by separable states. The three-mode state is prepared by overlapping a squeezed state, a vacuum state, and a thermal state at two balanced beam splitters. This step is analogous to the interference of modes  $A$  and  $C$  in the original protocol [7], and the state preparation procedure does not create any entanglement between mode  $B$  and modes  $A$  and  $C$ . After modes  $A$  and  $C$  have been sent to Alice and mode  $B$  has been sent to Bob, the  $B|AC$  and  $C|AB$  separability is carefully checked with balanced homodyne detectors  $BHD_A$ ,  $BHD_B$ , and  $BHD_C$ . Subsequently, Alice sends separable mode  $C$  to Bob. By overlapping modes  $C$  and  $B$  at another balanced beam splitter  $BS_3$ , entanglement is established between Alice and Bob, which is verified by balanced homodyne detectors  $BHD_A$  and  $BHD_{B'}$ . For details on the squeezed-light source and the generation of the thermal state, see the Supplemental Material [20].

using the homodyne detectors  $BHD_A$  and  $BHD_{B'}$ . Here,  $\hat{X}$  and  $\hat{P}$  describe the amplitude and phase quadrature operators, respectively. They are normalized to the shot noise level, i.e.,  $\text{Var}(\hat{X}) = \text{Var}(\hat{P}) = 1$  for a vacuum state. With our setup as described above, the protocol of entanglement distribution by separable states gets an intuitive view: correlated classical noise mixed into modes  $B$  and  $C$  restricts the entanglement to just one of the three bipartite splittings. By quantum interference at Bob's side, the classical noise can be removed and the distributed two-mode entangled state be created.

For investigating the separability properties of the three-mode state ( $ABC$ ), we apply the positive partial transposition criterion (PPT) [17,18] to the measured state. This criterion is both necessary and sufficient for bipartite splittings of Gaussian states with  $N$  modes with only a single mode on one side ( $1|N-1$ ) [19]. The three-mode state is separable with respect to mode  $k$  if the corresponding covariance matrix of the partially transposed state  $\gamma^{T(k)}$  fulfills the uncertainty relation

$$\gamma^{T(k)} - i\Omega \geq 0, \quad (2)$$

with  $\Omega = \bigoplus_{k=1}^3 J$ , where  $J = \begin{pmatrix} 0 & -1 \\ 1 & 0 \end{pmatrix}$ . This criterion is equivalent to finding the symplectic eigenvalues of the covariance matrix of the partially transposed state. If the smallest symplectic eigenvalue  $\mu_k$ , in the following called a PPT value, is below 1, the state is inseparable with respect to the  $k|ij$  splitting. For details, see the Supplemental Material [20].

We named the PPT values for the different splittings after the single mode:  $\text{PPT}_A$  for the ( $A|BC$ ) splitting,  $\text{PPT}_B$  for ( $B|AC$ ), and  $\text{PPT}_C$  for ( $C|AB$ ). Our protocol thus requires  $\text{PPT}_A < 1$  (= inseparable) and  $\text{PPT}_B, \text{PPT}_C > 1$  (= separable) to verify the appropriate three-mode state for distributing entanglement by separable states.

Within our experimental setup, we can vary the following critical parameters: the variance of the thermal state as well as the variances of the squeezed and antisqueezed quadratures of the squeezed state. The latter two can be changed independently of each other by variation of the pump power of the squeezed-light source and by variation of additional losses.

We performed theoretical simulations to analyze the influence of the squeezed and thermal states on the separability properties of the generated three-mode state. Figure 3 shows the  $\text{PPT}_C$  value of the three-mode state versus the noise power of the thermal state. Because of the symmetry of the setup,  $\text{PPT}_B$  and  $\text{PPT}_C$  are identical. The  $\text{PPT}_A$  value is not depicted, since this value is always below 1 when a squeezed state is used.

The magenta lines show that the property of separability is independent of the initial squeezing value. Hence, the amount of classical noise necessary to prohibit entanglement only depends on the optical loss applied to the

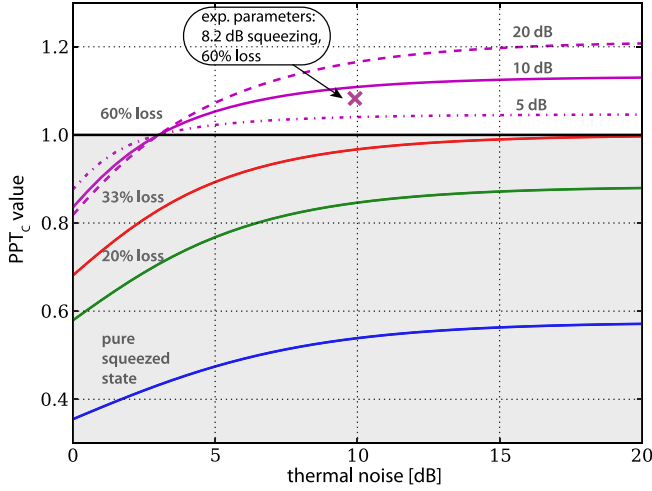


FIG. 3 (color online). Separability analysis. Theoretical simulations of the  $PPT_C$  value with respect to the added thermal noise (given in dB above vacuum noise variance) are depicted. The solid lines correspond to 10 dB initial squeezing with different losses. To obtain the required PPT value ( $> 1$ ), a minimal loss of 33% is necessary. The point of intersection with the threshold of 1 is exclusively depending on the loss and not on the actual initial squeezing value. The parameters, which were used in our measurements, are marked with the magenta cross.

squeezed state. Nevertheless, with higher squeezing values, the three-mode state is farther pushed into the separable regime with respect to the  $B|AC$  and  $C|AB$  splittings for a sufficiently “hot” thermal state. Apart from that, higher squeezing values result in stronger entanglement that is distributed between the two parties.

From Fig. 3, it is also visible that the entanglement can only be prevented by classical noise if the optical loss applied to the squeezed state is larger than 33.3%. This is exactly the threshold for which the bipartite entangled state, generated by the superposition of the squeezed and the vacuum states, is no longer Einstein-Podolsky-Rosen entangled [21]. Einstein-Podolsky-Rosen-entangled states are a subclass of general entanglement, exhibiting stronger quantum correlations. Indeed, the properties of our three-mode state show that these correlations are so strong that the entanglement in the bipartite splittings cannot be prevented by classical noise.

The 21 independent elements of the symmetric  $6 \times 6$  three-mode covariance matrix were determined from homodyne measurements on modes  $A$ ,  $B$ , and  $C$ . For each quadrature measurement, we recorded  $10^6$  data points. As input states, we used a squeezed state with  $-1.8$  and  $5.1$  dB noise reduction or amplification in the amplitude and phase quadrature, respectively, and an elliptical thermal state (“hot squeezed state”) with  $9.6$  and  $10.2$  dB noise amplification. The resulting three-mode covariance matrix  $\gamma$  was measured as

$$\gamma = \begin{pmatrix} 0.76 & 0.04 & 0.12 & -0.03 & 0.19 & -0.07 \\ 0.04 & 2.20 & 0.05 & -0.78 & -0.10 & -0.74 \\ 0.12 & 0.05 & 5.70 & -0.29 & -3.92 & 1.14 \\ -0.03 & -0.78 & -0.29 & 6.84 & -0.96 & -3.94 \\ 0.19 & -0.10 & -3.92 & -0.96 & 4.73 & 0.09 \\ -0.07 & -0.74 & 1.14 & -3.94 & 0.09 & 5.92 \end{pmatrix}.$$

This covariance matrix directly leads to the PPT values  $PPT_A = 0.89$ ,  $PPT_B = 1.1$ , and  $PPT_C = 1.07$ . Thus, the measured state fulfilled the requirements for distributing entanglement via separable states.

Three main effects could in principle cause the masking of the actual presence of entanglement. Two of them can also lead to a non-Gaussian state and can thus prohibit the application of the separability criterion for Gaussian states: phase fluctuations due to imperfect phase locking between signal beams and local oscillator beams and the generation of the thermal state by random displacements of originally squeezed states, where the distribution of random displacements can be non-Gaussian. These effects are considered in detail in the Supplemental Material [20] with the result that none of them has any non-negligible effect in the presented measurement.

The third effect is the influence of detection losses. Since we are in fact interested in the separability properties of the state *before* homodyne detection, the optical loss introduced by the measurement devices has to be computationally eliminated. Indeed, the separability properties of the state can be altered by a nonperfect detection process as depicted in Fig. 4. The magenta curves represent the  $PPT_B$  and  $PPT_C$  values of the covariance matrix  $\gamma$ , if optical loss within the homodyne detection is subtracted. The vertical black lines mark the regime of our estimated detection efficiency (quantum efficiency + visibility). We estimate the quantum efficiency of the homodyne detector’s photodiodes to be about 90%. The visibilities of the homodyne detectors were measured before each measurement and laid in a regime of 93%–98%. For the covariance matrix  $\gamma$ , the detection losses are thus  $11\% \pm 5\%$  for the homodyne detector  $BHD_A$ ,  $17\% \pm 5\%$  for  $BHD_B$ , and  $16.6\% \pm 5\%$  for  $BHD_C$ , which leads to a lower bound of 6% and an upper bound of 22% loss. After subtracting the losses from the three-mode covariance matrix, the lower and upper bounds for the PPT values are 0.85 and 0.87 for the  $A|BC$  splitting, 1.07 and 1.09 for the  $B|AC$  splitting, and 1.04 and 1.06 for the  $C|AB$  splitting and thus fulfill the criteria. This shows the correctness of the separability properties regardless whether the detection loss is considered to be part of the detected state or not.

Monte Carlo simulations showed that for the  $10^6$  measurements per homodyne setting, the statistical error bars on the symplectic eigenvalues are of the order of 0.001. That means that the inferred separability properties are statistically reliable even for the extreme limit of 22% loss.

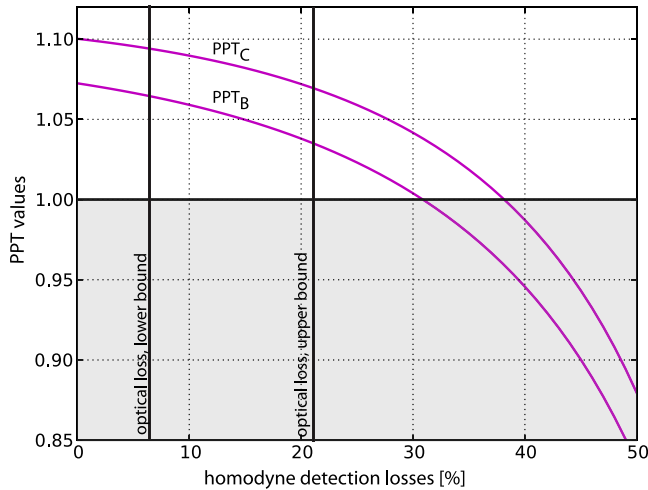


FIG. 4 (color online). Measured PPT values with subtraction of detection losses. The magenta curves show the inferred  $\text{PPT}_B$  and  $\text{PPT}_C$  values of the measured covariance matrix  $\gamma$  for a spectrum of computationally eliminated detection losses. Based on independent measurements, we estimate the actual detection loss to be greater 7% and smaller 22%. These losses do not push the PPT values below unity. The successful demonstration of our protocol is thus independent of the question of whether detection loss should be corrected for or not.

After the prepared three-mode state had been checked for its separability properties, ancilla mode  $C$ , which was separable from modes  $A$  and  $B$ , was sent to Bob. Two-mode entanglement between Alice and Bob was generated by superimposing modes  $C$  and  $B$  at the balanced beam splitter  $\text{BS}_3$  with the appropriate phase, which was controlled manually. The criterion by Duan *et al.* resulted in 3.4 ( $< 4$ ), which proved that entanglement was successfully distributed by separable states.

In conclusion, we experimentally realized entanglement distribution by separable states. We showed that for this protocol, a specific three-mode state is suitable, whose thermal noise prevented entanglement in two of the three bipartite splittings. After transmission of a separable state, entanglement was revealed via quantum interference. We could show that the protocol does not work with Einstein-Podolsky-Rosen-entangled states, since with states of this class of entanglement, separability cannot be enforced by introducing thermal noise. While the entanglement distribution by separable states seems counterintuitive in the first place, our experiment provides an insight into the underlying physical mechanism behind this protocol. From a broader perspective, our work helps to understand the possibilities and restrictions offered by multimode entangled quantum states and future multipartite quantum communication networks. Our implementation also clearly demonstrates the experimental feasibility of removing classical noise from a decohered entangled state by quantum interference if the classical noise is correlated in two modes.

This research was supported by the FP7 Project QESSENCE (Grant Agreement No. 248095) and the Centre for Quantum Engineering and Space-Time Research (QUEST). We thank the IMPRS on Gravitational Wave Astronomy for support. V.H. acknowledges support from HALOSTAR. J.F. acknowledges support from the Czech Science Foundation under Project No. P205/12/0694 and from the European Social Fund and MSMT under Project No. EE2.3.20.0060.

*Note added.*—Recently, we became aware of another two successful demonstrations of entanglement distribution by separable states, with continuous as well as with discrete variables, respectively [22,23].

\*Corresponding author.

roman.schnabel@aei.mpg.de

- [1] H. J. Kimble, *Nature (London)* **453**, 1023 (2008).
- [2] R. Horodecki, P. Horodecki, M. Horodecki, and K. Horodecki, *Rev. Mod. Phys.* **81**, 865 (2009).
- [3] T. S. Cubitt, F. Verstraete, W. Dür, and J. I. Cirac, *Phys. Rev. Lett.* **91**, 037902 (2003).
- [4] G. Giedke, B. Kraus, M. Lewenstein, and J. I. Cirac, *Phys. Rev. A* **64**, 052303 (2001).
- [5] T. K. Chuan, J. Maillard, K. Modi, T. Paterek, M. Paternostro, and M. Piani, *Phys. Rev. Lett.* **109**, 070501 (2012).
- [6] A. Kay, *Phys. Rev. Lett.* **109**, 080503 (2012).
- [7] L. Mišta and N. Korolkova, *Phys. Rev. A* **77**, 050302 (2008).
- [8] S. L. Braunstein and P. van Loock, *Rev. Mod. Phys.* **77**, 513 (2005).
- [9] A. Furusawa, J. L. Sorensen, S. L. Braunstein, C. Fuchs, H. J. Kimble, and E. S. Polzik, *Science* **282**, 706 (1998).
- [10] W. P. Bowen, N. Treps, B. C. Buchler, R. Schnabel, T. C. Ralph, H.-A. Bachor, T. Symul, and P. K. Lam, *Phys. Rev. A* **67**, 032302 (2003).
- [11] V. Scarani, H. Bechmann-Pasquinucci, N. Cerf, M. Dušek, N. Lütkenhaus, and M. Peev, *Rev. Mod. Phys.* **81**, 1301 (2009).
- [12] Z. Zhao, T. Yang, Y.-A. Chen, A.-N. Zhang, M. Zukowski, and J.-W. Pan, *Phys. Rev. Lett.* **91**, 180401 (2003).
- [13] R. Raussendorf and H. J. Briegel, *Phys. Rev. Lett.* **86**, 5188 (2001).
- [14] P. Walther, K. J. Resch, T. Rudolph, E. Schenck, H. Weinfurter, V. Vedral, M. Aspelmeyer, and A. Zeilinger, *Nature (London)* **434**, 169 (2005).
- [15] R. Ukai, N. Iwata, Y. Shimokawa, S. C. Armstrong, A. Politi, J. Yoshikawa, P. van Loock, and A. Furusawa, *Phys. Rev. Lett.* **106**, 240504 (2011).
- [16] L. M. Duan, G. Giedke, J. I. Cirac, and P. Zoller, *Phys. Rev. Lett.* **84**, 2722 (2000).
- [17] M. Horodecki, P. Horodecki, and R. Horodecki, *Phys. Lett. A* **223**, 1 (1996).
- [18] R. Simon, *Phys. Rev. Lett.* **84**, 2726 (2000).
- [19] R. F. Werner and M. M. Wolf, *Phys. Rev. Lett.* **86**, 3658 (2001).

- [20] See Supplemental Material at <http://link.aps.org/supplemental/10.1103/PhysRevLett.111.230505> for details on the covariance matrix, verification of separability, statistical errors, and experimental techniques.
- [21] T. Eberle, V. Händchen, J. Duhme, T. Franz, R. F. Werner, and R. Schnabel, *Phys. Rev. A* **83**, 052329 (2011).
- [22] C. Peuntinger, V. Chille, L. Mišta, N. Korolkova, M. Förtsch, J. Korger, C. Marquardt, and G. Leuchs, following Letter, *Phys. Rev. Lett.* **111**, 230506 (2013).
- [23] A. Fedrizzi, M. Zuppardo, G. G. Gillett, M. A. Broome, M. de Almeida, M. Paternostro, A. G. White, and T. Paterek, preceding Letter, *Phys. Rev. Lett.* **111**, 230504 (2013).